Experimental and Computer Simulation Analysis of a Gunn Diode

YUKIO ITO, SENIOR MEMBER, IEEE, HIDEMITSU KOMIZO, TAKESHI MEGURO, YOSHIMASA DAIDO, AND ITSUO UMEBU

Abstract—Bias-voltage and frequency dependencies of large signal electronic admittance of a Gunn diode have been measured systematically in the 8- to 13-GHz frequency range. The results were qualitatively verified by computer simulation. These results furnished information which was useful in the direct design of broad-band injection-locked oscillators and amplifiers. The results also gave a better understanding of irregular phenomena commonly observed in conventional oscillators.

I. Introduction

THE DEVELOPMENT of Gunn diode oscillators for large-capacity microwave communication equipment presents many problems. Among these are hysteresis phenomena as well as instabilities in a cavity stabilized oscillator, a broad-band injection-locked oscillator, and other Gunn diode circuits.

To solve these problems, it is necessary to determine and apply the precise dynamic electronic admittance of a Gunn diode and its bias-voltage and frequency dependencies, to the design of the appropriate circuit.

Many authors have studied dynamic behavior of Gunn diode through computer simulation. They usually simulated the long Gunn diodes [1]–[4] (30 to 200 μm), with the exception of 10-μm diodes under RF short-circuit conditions [5]. However, none of these authors' results is suitable to solve the circuit design problem mentioned above. A 10-μm long Gunn diode has been simulated, with nonideal electrodes under various RF circuit conditions, and the electronic admittance of a Gunn diode in the X band was obtained.

Also described is the large signal electronic admittance of a Gunn diode, measured in a coaxial mount at various operating bias voltages beyond the threshold voltage in the frequency range from 8 to 13 GHz.

Such characteristics as electronic admittance slope, corresponding frequency dependency, and output power are discussed. Measured values are compared with results of the computer simulation.

This presentation shows that measured electronic admittance very nearly coincided with calculated values.

Manuscript received April 30, 1971; revised July 19, 1971.

Y. Ito, H. Komizo, T. Meguro, and Y. Daido are with the Radio Transmission Laboratory, Fujitsu Laboratories Ltd., Kawasaki, Japan.

I. Umebu is with the Semiconductor Laboratory, Fujitsu Laboratories Ltd., Kawasaki, Japan.

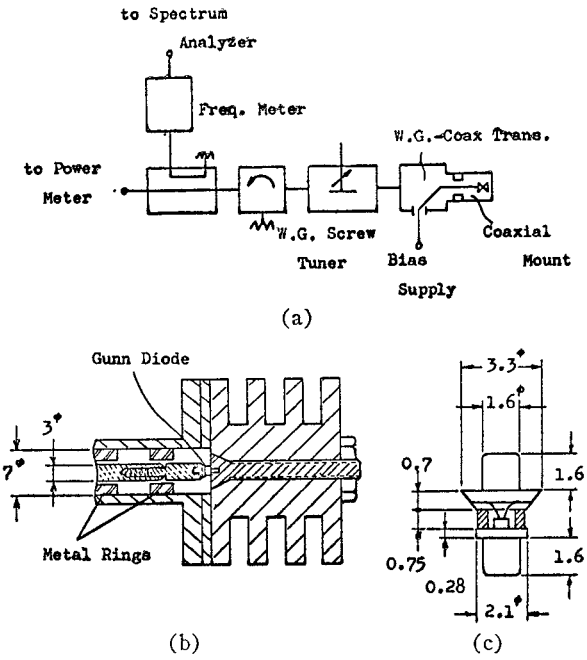

Fig. 1. (a) Measuring setup. (b) Cross-sectional view of the coaxial mount. (c) Packaged diode dimensions (in millimeters).

II. Electronic Admittance Measurement

Measured diode admittance of a packaged Gunn diode mounted in a waveguide has been reported [6] with regard to the design of a cavity-stabilized Gunn oscillator. However, the equivalent circuit of a Gunn diode mounted in a waveguide is too complicated to eliminate parasitic elements from measured diode admittance through calculations.

This prevents accurately calculating electronic admittance. Thus, a coaxial mount [shown in Fig. 1(b)] was used which permitted precise admittance measurement over a wide frequency range, from 8 to 13 GHz.

Fig. 1(a) shows the block diagram for diode admittance measurement and Fig. 1(c) shows packaged diode dimensions. The coaxial mount has two movable metal rings for impedance matching. DC bias voltage is externally supplied through an RF choke in the WG–coaxial transition. A standard pill-type packaged Gunn diode was placed at the end of the coaxial line ($Z_0 = 50\,\Omega$) with a good heat sink.

Several diodes from one production lot (made by Fujitsu Laboratories Ltd.) have been used in this ex-

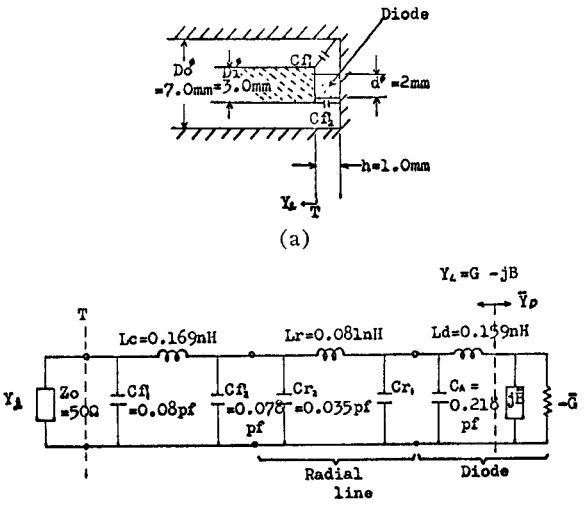

D_0, D_1, d diameter of the outer conductor; inner conductor of the coaxial line; and packaged Gunn diode, respectively;
C_{f1}' fringing capacitance from the corner of the center conductor to the outer conductor;
C_{f2}' fringing capacitance between the corner of the center conductor and terminal plane of the mount,
$-\bar{G}, j\bar{B}$ negative conductance and susceptance of Gunn diode, respectively;
L_d inductance of the internally short-circuited diode package;
C_A parallel capacitance of the diode without active layer;
L_c, L_r, C_{r1}, C_{r2} inductance and capacitance produced in the coaxial sections of the mount;
Y_l load admittance looking from T-plane.

Fig. 2. (a) Schematic diagram of the coaxial mount. (b) Its equivalent circuit looking from T-plane.

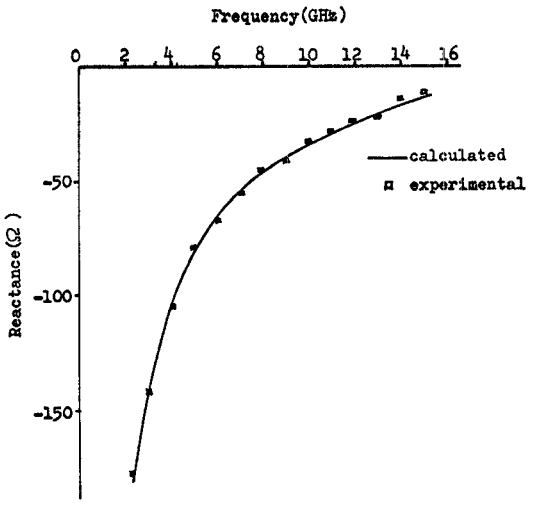

Fig. 3. Experimental verification of the equivalent circuit shown in Fig. 2(b) in the case of an open diode. The curve shows the calculated reactance value using the equivalent circuit shown in Fig. 2(b). Open squares show measured values.

periment. Each diode has a mesa construction with n^+-n-n^{++} layers and the n^{++} cap is upside-down bonded to the heat sink.

The n epitaxial layer was grown by the vapor phase method. Carrier concentration is about 1.0×10^{15}–3.0×10^{15} cm^{-3} (the doping profile has a positive gradient from cathode to anode and there are some local fluctuations on one wafer). The active layer has a cross-sectional area of about 2×10^4 μm^2 and about a 10-μm thickness. The threshold voltage of these Gunn diodes is about 3.0 V.

At operating bias voltages of 5.5, 7.0, and 8.9 V, oscillating frequency and output power are adjusted by sliding the metal rings and by tuning the waveguide screw tuner. A spectrum analyzer was used to check the noise spectrum and single oscillation (no harmonic oscillations). Figs. 2(a) and (b) show the schematic diagram of the coaxial mount and its equivalent circuit, proposed by Getsinger [7].

After adjustment, the diode was replaced with a measurement adaptor and the load admittance Yl was measured using the coaxial slotted line from the diode electrode as the reference plane [T plane in Fig. 2(a)]. Packaged diode admittance Y_d [packaged diode admittance Y_d (including the parasitic elements of the package)] was then determined by applying negative sign to Yl, i.e., $-Yl$.

Large signal electronic admittance $\bar{Y}_D$ can be calculated by subtracting parasitic admittance of the packaged diode from $-Yl$. There may be some differences in $\bar{Y}_D$ between diodes and also some measurement error. Thus, from more than 3000 measured values, we plotted the maximum common $\bar{G}$–$\bar{B}$ curve for each operating frequency.

Diode lead inductance L_d was measured at the low frequency of 1 GHz, where the effect of the parallel susceptance produced by capacitance C_A is negligible, with a short-circuited diode (no active layer), using a dummy diode (metal block) as a reference plane. Parallel capacitance C_A is $C_A'+C_d$, where C_A' represents the difference between mount capacitance measured with an open-circuited package in place in the mount, and mount capacitance measured using only the end caps instead of the open diode package; C_d (parallel-plate capacitance) is calculated from the relationship $C_d=\pi d^2\epsilon_0/4h$.

From the relationships shown in [7], the other parasitic elements produced in the radial section of the mount, such as L_r, L_c, C_{r1}', C_{r2}', C_{f1}, and C_{f2}, were calculated. Resultant parasitic element values are shown in the equivalent circuit in Fig. 2(b). The equivalent circuit was verified at several frequencies up to 15 GHz by passive impedance measurements, using an open-circuited package. Fig. 3 shows the measured and calculated reactance values.

From Fig. 3, a good agreement between them can be seen in the frequency range below 13 GHz. Above 13 GHz, the error gradually increases and becomes about 20 percent at 15 GHz. Also, the calculated reactance values using the equivalent circuit very closely coincides with the detail experimental results in Fig. 4 of [8], in which almost the same dimensional package as shown in Fig. 1(c) was used. In this case, series resistance of the Gunn diode is included in electronic admittance $\bar{Y}_D$.

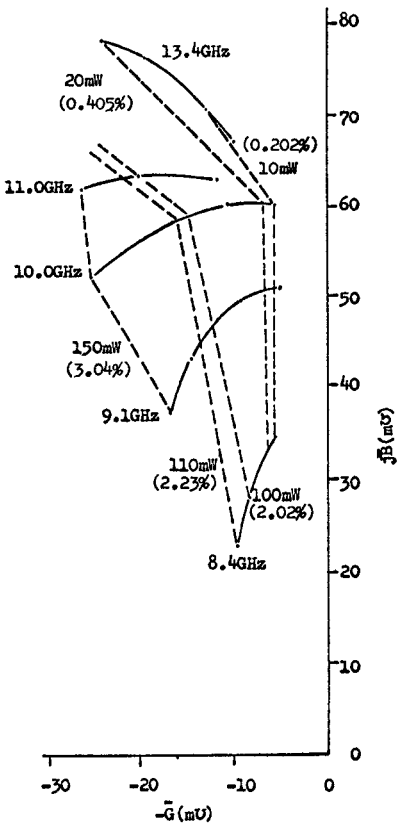

Fig. 4. Measured electronic admittance for bias voltage of 8.9 V. Solid lines show electronic admittance. Dashed lines show equal output power lines. Figures in parentheses show efficiency.

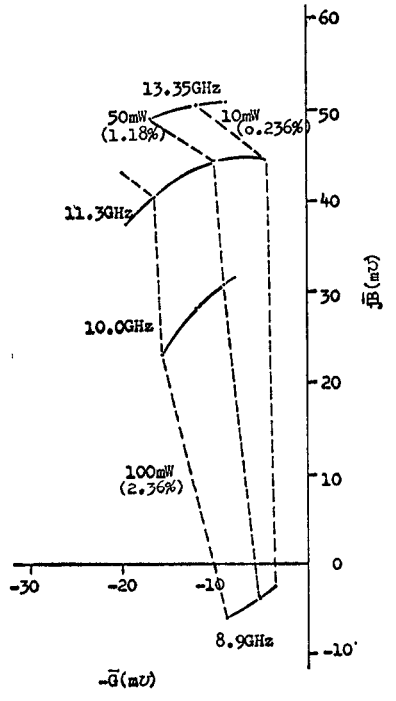

Fig. 5. Measured electronic admittance for bias voltage of 7.0 V. Solid lines show electronic admittance. Dashed lines show equal output power lines. Figures in parentheses show efficiency.

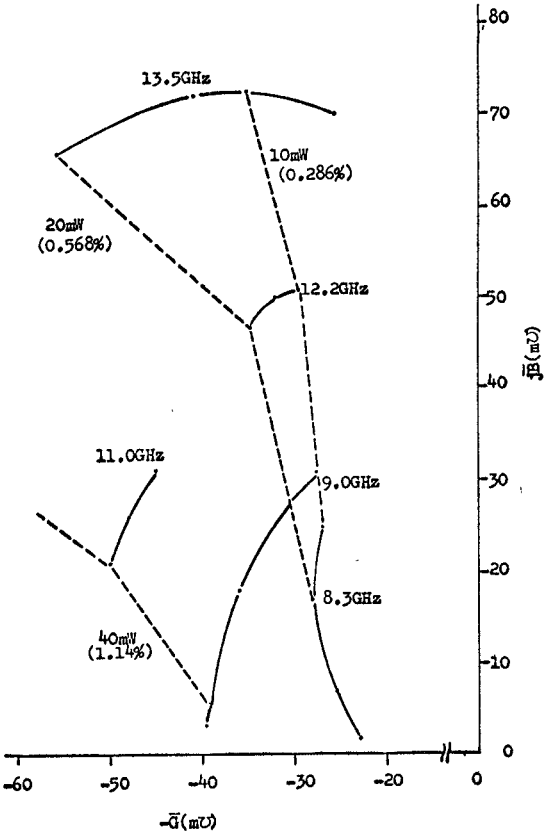

Fig. 6. Measured electronic admittance for bias voltage of 5.5 V. Solid lines show electronic admittance. Dashed lines show equal output power lines. Figures in parentheses show efficiency.

Figs. 4, 5, and 6 show measured electronic admittance $\overline{Y}_D$ for bias voltages of 5.5, 7.0, and 8.9 V as a frequency parameter. Each solid line indicates $\overline{G}$–$\overline{B}$ curve, and points on the dashed line have equal output power values. The figures show output power delivered to the load in milliwatts. The figures in parentheses show efficiency.

Fig. 7 shows the normalized ($Z_0 = 50\ \Omega$) electronic admittance $\overline{Y}_D (= \overline{G} + j\overline{B})$ and packaged diode admittance $\overline{Y}_d (= \overline{G}_d + j\overline{B}_d)$ on a Smith chart, for 8.9-V bias voltage. The packaged diode has a series resonance at about 9.0 GHz.

III. Computer Simulation

Computer simulations of Gunn diodes are made for the one-dimensional model illustrated in Fig. 8. It has a 9-μm uniformly doped active layer, exponentially varying transient regions (about 2.4 μm in length each) and electrodes (1 μm in length each) which are doped 10 times as highly as the active layer.

Transient phenomena of the high field domain must have significant effects on the performance of these diodes. This model has a passive series resistance near electrodes which is estimated about at 10 percent to the

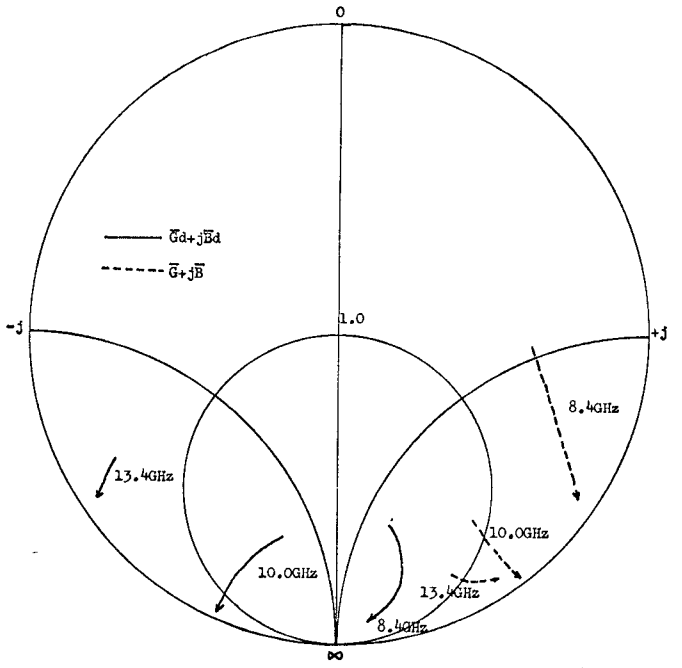

Fig. 7. Electronic admittance $\bar{Y}_D(=\bar{G}+j\bar{B})$, and diode admittance $\bar{Y}_d(=\bar{G}d+j\bar{B}d)$, including parasitic elements of the package, for 8.9-V bias voltage.

low field resistance of the diode. But the computer simulations show that the series resistance of this order hardly affects the oscillation efficiencies and admittances.

The notch in the active layer is 20 percent in depth, 1 μm in length, and it is located 0.5 μm from the end of the exponential region of the cathode side. The domain is known to disappear at about 1 μm within the exponential region of the anode side in this model.

The basic equations for the simultations are

$$\epsilon \frac{\partial E}{\partial t} = q(n - n_0) \tag{1}$$

$$J = qnv - qD\frac{\partial n}{\partial x} + \epsilon\frac{\partial E}{\partial t} \tag{2}$$

where ϵ: dielectric constant of GaAs $12.5\times8.854\times10^{-12}$ F/m, E: the electric field in the diode, q: electronic charge 1.6021×10^{-19} C, n: electron density, n_0: donor density, J: total current, v: electron drift velocity, and D: diffusion coefficient of electron 200 cm^2/s (which is assumed constant). The drift velocity of electrons is assumed as the instantaneous function of the electric field and has the form [3]

$$v = \frac{\mu E + v_s(E/E_0)^4}{1 + (E/E_0)^4} \tag{3}$$

where μ: low field mobility 8000 cm^2/V·s, v_s: saturation velocity 8.5×10^6 cm/s, and $E_0=4000$ V/cm. The

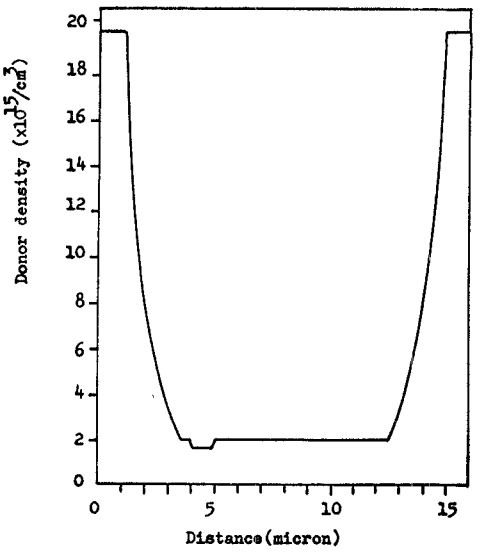

Fig. 8. Doping profile used in the simulation of Gunn diodes.

boundary conditions are

$$\frac{\partial E}{\partial x} = 0 \qquad \text{at } x = 0 \quad \text{and} \quad x = L \tag{4}$$

$$-\int_0^L Edx = V_{dc} + V_{RF}\sin(2\pi f) \tag{5}$$

where L is the sample length, V_{dc} is the bias voltage, V_{RF} is the RF voltage induced in the resonance circuit, and f is the oscillation frequency. Equations (1) and (2) are solved under boundary conditions (4), (5) and proper initial conditions by FACOM 230-60 computer system. The donor density of the active layer is chosen as 2×10^{15} cm^{-3} throughout this paper. Low field resistance is 2.2 Ω and the series resistance is estimated at about 0.2 Ω for cross-sectional area 2×10^4 μm^2.

Under the RF short-circuit condition, the transient time of the high field domain reaches one-half of the current waveform periods and the repetition frequency of the domain becomes 9.8–10.5 GHz for a bias voltage of 8.9–5.5 V. Simulation of Gunn diodes under the parallel resonance circuit are made for frequencies of 8, 10, and 12 GHz. Bias voltages are 5.5, 7.0, and 8.9 V in accordance with experiments and RF voltages are chosen for the electric field of diodes to be swung fully down to the threshold and/or sustaining fields. If we choose the smaller RF voltages, the simulation doesn't give a stationary solution.

Representative electronic current waveforms for three frequencies are shown in Fig. 9.

Admittances of the Gunn diodes together with efficiencies and output power (figures in parentheses) are shown in Fig. 10, for 8.9-V bias voltage as an example. Fig. 11 shows the calculated electronic admittance for 10 GHz as a parameter of 5.5-, 7.0-, and 8.9-V bias voltages.

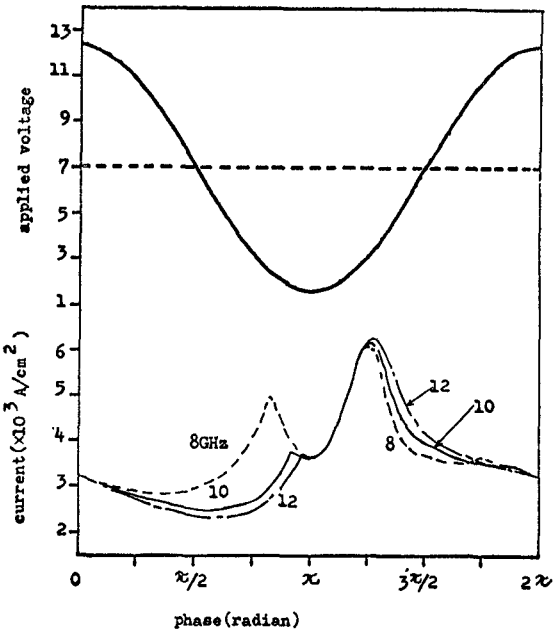

Fig. 9. Electronic current waveforms and voltage waveform; $V_{op}=7.0$ V, $V_{RF}=5.4$ V. Figures show frequency in GHz.

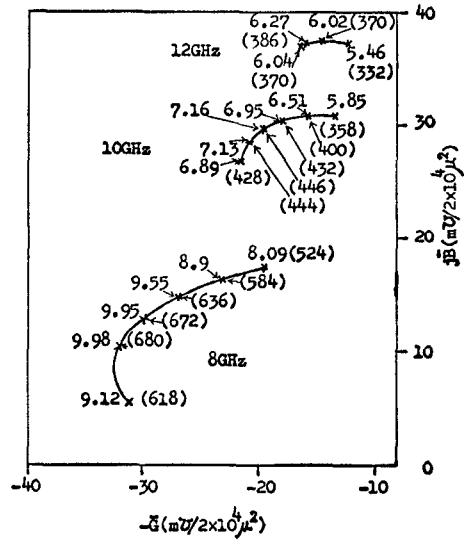

Fig. 10. Calculated electronic admittance for 8.9-V bias voltage. Figures show efficiency and figures in parentheses show output power in milliwatt per 2×10^4-μm^2 area.

IV. Results and Discussion

From the results of experiments and computer simulation, we can clearly distinguish many important characteristics of a Gunn diode. The following agreements exist between the experiment and simulation results.

1) Admittance slope $\partial\overline{B}/\partial|\overline{G}|$ changes clockwise with frequency.

2) At constant frequency and bias voltage, output power tends to increase as negative conductance increases, although, in the simulation, maximum output power is observed at a certain negative conductance, as shown in Fig. 10.

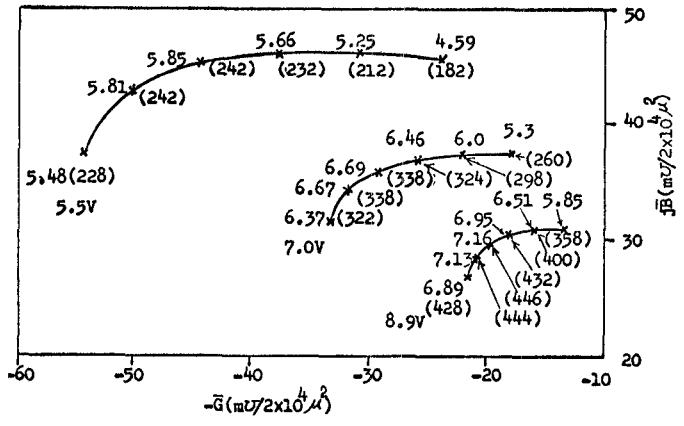

Fig. 11. Calculated electronic admittance for 10-GHz frequency. Figures show efficiency and figures in parentheses show output power in milliwatt per 2×10^4-μm^2 area.

3) On the order of $|\overline{G}|$ and $|\overline{B}|$, especially good agreement can be seen in the value of $|\overline{G}|$.

4) $|\overline{B}|$ increases with frequency.

5) As the bias voltage becomes larger up to 7.0 V, $|\overline{G}|$ and $|\overline{B}|$ seem to converge to the origin.

On the other hand, the following disagreements exist between them.

1) In the experimental results, maximum power appears in the frequency range of 9–11 GHz and output power drops sharply at higher frequencies for constant bias voltage. However, in the simulation result, output power increases inversely to frequency in the frequency range of 8 to 12 GHz.

2) In the experimental results $|\overline{G}|$ and $|\overline{B}|$ increase as bias voltage increases at a higher than 7.0-V bias voltage. This means that the diodes used have negative slopes at the oscillating frequency with respect to bias voltage. A similar relationship was observed for temperature through temperature tests [6]. In the simulation results, $|\overline{G}|$ and $|\overline{B}|$ decrease gradually with bias voltage.

3) In the experimental results, capacitive susceptance $\overline{B}$ becomes zero at about 9.0 GHz at a 7.0-V bias voltage (which suggests a parallel resonance of the electronic admittance), as shown in Fig. 5. But this is not observed in the simulation results, at least in the frequency range of 8 to 12 GHz.

4) Calculated output power and efficiency are about 2–3 times larger than measured ones.

5) The theoretical model must assume an RF voltage sufficient to swing the total device voltage down to threshold value. However, the RF voltage values by simple calculation from the experimental $\overline{G}$–$\overline{B}$ curves and output power show that the RF voltage values are much smaller (do not swing to below threshold voltage).

The reasons for such disagreements are presumed to be as follows for items 1), 2), 3), and 4).

1) There is a difference of doping profile between the theoretical model and the actual diodes.

2) The thermal effect which is not taken into account in simulation cannot be negligible in the actual diode.

For item 5) in actual operation it is not clear whether the RF voltage swings down to the threshold voltage or not. But the following two different explanations can be considered as reasons for this disagreement.

1) Gunn diodes have nonlinear susceptance, which varies with the change of bias voltage, so that the RF voltage of the active layer may be unsymmetric in positive and negative half cycle. Then there is a possibility that, although the first harmonics of RF voltage are not sufficiently large, the total RF voltage may swing down to threshold voltage.

2) In the actual Gunn diodes, the doping profiles have fluctuations, therefore the multidomain effect can possibly occur. In this case the RF voltages are not necessarily large enough. However, it is difficult to treat a multidomain model systematically in simulation.

V. Conclusion

The bias voltage and frequency dependency of large signal electronic admittance of a Gunn diode were measured in detail and results were qualitatively verified through computer simulation. Comparison between the measured and simulation results have been discussed. Some disagreements exist between them, but the reasons for these disagreements are not clear at present. A further detailed investigation will be necessary. The results presented here furnished useful information for a direct circuit design of Gunn oscillators and amplifiers and gave a better understanding of Gunn diode behavior.

Acknowledgment

The authors wish to thank Dr. S. Kojima, Managing Director, F. Iwai and Dr. H. Yunoki, Managers of the Radio Transmission Laboratory, and Dr. T. Oshida and Dr. I. Tsurumi, Managers of the Semiconductor Laboratory, Fujitsu Laboratories Ltd., for their encouragement during this study; and F. Takanashi, S. Yanagisawa, H. Ashida, and H. Sumi for their helpful discussion and assistance.

References

[1] D. E. McCumber and A. G. Chynoweth, "Theory of negative-conductance amplification and of Gunn instabilities in 'two-valley' semiconductors," *IEEE Trans. Electron Devices*, vol. ED-13, Jan. 1966, pp. 4–27.

[2] H. Kroemer, "Nonlinear space-charge domain dynamics in a semiconductor with negative differential mobility," *IEEE Trans. Electron Devices*, vol. ED-13, Jan. 1966, pp. 27–40.

[3] H. W. Thim, "Computer study of bulk GaAs devices with random one-dimensional doping fluctuations," *J. Appl. Phys.*, vol. 39, July 1968, pp. 3897–3904.

[4] R. B. Robrock, II, "Analysis and simulation of domain propagation in nonuniformly doped bulk GaAs," *IEEE Trans. Electron Devices*, vol. ED-16, July 1969, pp. 647–653.

[5] M. Suga and K. Sekido, "Effects of doping profile upon characteristics of Gunn Diodes," *IEEE Trans. Electron Devices*, vol. ED-17, Apr. 1970, pp. 275–281.

[6] Y. Ito, H. Komizo, and S. Sasagawa, "Cavity stabilized *X*-band Gunn oscillator," *IEEE Trans. Microwave Theory Tech.*, vol. MTT-18, Nov. 1970, pp. 890–897.

[7] W. J. Getsinger, "The packaged and mounted diode as a microwave circuit," *IEEE Trans. Microwave Theory Tech.*, vol. MTT-14, Feb. 1966, pp. 58–69.

[8] I. W. Pence and P. J. Khan, "Broad-band equivalent-circuit determination of Gunn diodes," *IEEE Trans. Microwave Theory Tech.*, vol. MTT-18, Nov. 1970, pp. 784–789.